

Brain and Testis Accumulation of Regorafenib is Restricted by Breast Cancer Resistance Protein (BCRP/ABCG2) and P-glycoprotein (P-GP/ABCB1)

Anita Kort · Selvi Durmus · Rolf W. Sparidans · Els Wagenaar · Jos H. Beijnen · Alfred H. Schinkel

Received: 26 September 2014 / Accepted: 12 December 2014 / Published online: 8 January 2015
© Springer Science+Business Media New York 2015

ABSTRACT

Purpose Regorafenib is a novel multikinase inhibitor, currently approved for the treatment of metastasized colorectal cancer and advanced gastrointestinal stromal tumors. We investigated whether regorafenib is a substrate for the multidrug efflux transporters ABCG2 and ABCB1 and whether oral availability, brain and testis accumulation of regorafenib and its active metabolites are influenced by these transporters.

Methods We used *in vitro* transport assays to assess human (h)ABCB1- or hABCG2- or murine (m)Abcg2-mediated active transport at high and low concentrations of regorafenib. To study the single and combined roles of Abcg2 and Abcb1a/1b in oral regorafenib disposition and the impact of Cyp3a-mediated metabolism, we used appropriate knockout mouse strains.

Results Regorafenib was transported well by mAbcg2 and hABCG2 and modestly by hABCB1 *in vitro*. Abcg2 and to a lesser extent Abcb1a/1b limited brain and testis accumulation of regorafenib and metabolite M2 (brain only) in mice. Regorafenib oral

availability was not increased in *Abcg2^{-/-};Abcb1a/1b^{-/-}* mice. Up till 2 h, metabolite M5 was undetectable in plasma and organs.

Conclusions Brain and testis accumulation of regorafenib and brain accumulation of metabolite M2 are restricted by Abcg2 and Abcb1a/1b. Inhibition of these transporters may be of clinical relevance for patients with brain (micro)metastases positioned behind an intact blood–brain barrier.

KEY WORDS ABCB1 · ABCG2 · brain accumulation · regorafenib · testis accumulation

ABBREVIATIONS

ABC	ATP-binding cassette
AUC	Area under the plasma concentration-time curve
BBB	Blood–brain barrier
BCRP	Breast cancer resistance protein
BTB	Blood–testis barrier
C _{max}	Maximum drug concentration in plasma
CNS	Central nervous system
GIST	Gastrointestinal stromal tumors
LLOQ	Lower limit of quantitation
LOD	Lower limit of detection
P-gp	P-glycoprotein
SD	Standard deviation
TKI	Tyrosine kinase inhibitor
T _{max}	Time after administration of a drug to reach maximum plasma concentration

Electronic supplementary material The online version of this article (doi:10.1007/s11095-014-1609-7) contains supplementary material, which is available to authorized users.

A. Kort · S. Durmus · E. Wagenaar · A. H. Schinkel (✉)
Division of Molecular Oncology, The Netherlands Cancer Institute, Plesmanlaan 121, 1066 CX Amsterdam, The Netherlands
e-mail: a.schinkel@nki.nl

R. W. Sparidans · J. H. Beijnen
Division of Pharmacoepidemiology & Clinical Pharmacology
Department of Pharmaceutical Sciences, Faculty of Science, Utrecht University, Universiteitsweg 99, 3584 CG Utrecht, The Netherlands

A. Kort · J. H. Beijnen
Department of Pharmacy & Pharmacology, The Netherlands Cancer Institute/Slotervaart Hospital, Plesmanlaan 121, 1066 CX Amsterdam, The Netherlands

J. H. Beijnen
Department of Clinical Pharmacology, The Netherlands Cancer Institute, Plesmanlaan 121, 1066 CX Amsterdam, The Netherlands

INTRODUCTION

Multidrug efflux transporters of the ATP-binding cassette (ABC) protein family can have important roles in drug disposition. This impact is especially relevant for anti-cancer drugs as these drugs are usually administered close to their maximum tolerated dose. ABCB1 (P-glycoprotein) and ABCG2

(BCRP) are expressed on the apical membrane of epithelia in a number of organs which are pivotal for absorption and elimination of drugs like liver, small intestine and kidney, but also on luminal membranes of barriers protecting sanctuary tissues like the blood-placenta, blood-testis and blood-brain barrier. At these sanctuary sites ABCB1 or ABCG2 substrates are immediately pumped out of the epithelial or endothelial cells back into the blood. As a consequence, only small amounts of drug can accumulate in, for instance, the brain to treat (micro)metastases that are present behind a functionally intact blood-brain barrier. Many anticancer drugs including tyrosine kinase inhibitors (TKIs) have been shown to be substrates of ABCG2 or ABCB1 or both by different research groups, resulting sometimes in a decreased oral availability and often in a decreased brain accumulation (1–3).

Regorafenib (BAY 73-4506, Stivarga, [Supplementary Materials](#)) is an orally dosed tyrosine kinase inhibitor targeting angiogenic, stromal and oncogenic receptor kinases, and currently being investigated for the treatment of multiple tumor types (4). In a phase III study in patients with metastasized colorectal carcinoma, regorafenib improved overall survival 6 months compared to placebo (5). This led to the approval of regorafenib by EMA and FDA in 2012. The indication for regorafenib use was recently expanded to advanced gastrointestinal stromal tumors (GIST), following a randomized double-blind placebo-controlled study of Demetri *et al.* (6,7). Progression-free survival and disease control rate were significantly improved by regorafenib in patients with advanced GIST whose tumors had developed resistance to imatinib and sunitinib (8).

Regorafenib (flurosorafenib) was developed as a more potent RAF-kinase inhibitor than sorafenib. These compounds have overlapping biochemical activities, however, regorafenib does not only have affinity for a broader range of antiangiogenic kinases (VEGFR1-VEGFR3) compared to sorafenib, it also targets TIE2 (tyrosine kinase with immunoglobulin and epidermal growth factor homology domain 2). The inhibition of both classes of kinases has been shown to act synergistically, resulting in a reduced tumor growth in pre-clinical models (9,10).

Furthermore, Bruix *et al.* found evidence for regorafenib antitumor activity in hepatocellular carcinoma patients that had previously been treated with sorafenib (11). Regorafenib was able to delay disease progression in 25 out of 31 patients and one patient exhibited a partial response. A phase III study is currently recruiting to further investigate this effect (ClinicalTrialsGov identifier NCT01774344).

Sorafenib has been reported by various groups to be a good substrate of ABCG2 and a moderate substrate of ABCB1 *in vitro* as well as *in vivo* (12–15). Considering the similarity in chemical structure of regorafenib and sorafenib ([Supplementary Materials](#), respectively) where regorafenib has an additional fluorine atom attached to the central aromatic

Fig. 1 *In vitro* transport of 5 μM regorafenib. Transepithelial transport of regorafenib (5 μM) was assessed in MDCK-II cells either nontransduced (**a, b**) or transduced with hABCB1 (**c, d**), mAbcg2 (**e, f**) or hABCG2 (**g, h**) cDNA. At $t = 0$ h, regorafenib was applied to the donor compartment and concentrations in the acceptor compartment were measured at $t = 2, 4$ and 8 h and plotted as total amount of transport (ng) in the graphs. (**b, d-h**) zosuquidar (5 μM) and/or Ko143 (5 μM) were applied as indicated to inhibit hABCB1 or hABCG2 and mAbcg2, respectively. r relative transport ratio. BA (\square , dashed line), translocation from basolateral to apical compartment; AB (\bullet , continuous line), translocation from apical to basolateral compartment. *, $P < 0.05$; ***, $P < 0.001$ indicates significant transepithelial transport at $t = 8$ h. Points, mean ($n = 3$); bars, SD. At $t = 8$ h, 1 nmol transport corresponds to an apparent permeability coefficient (P_{app}) of 6.2×10^{-6} cm/s.

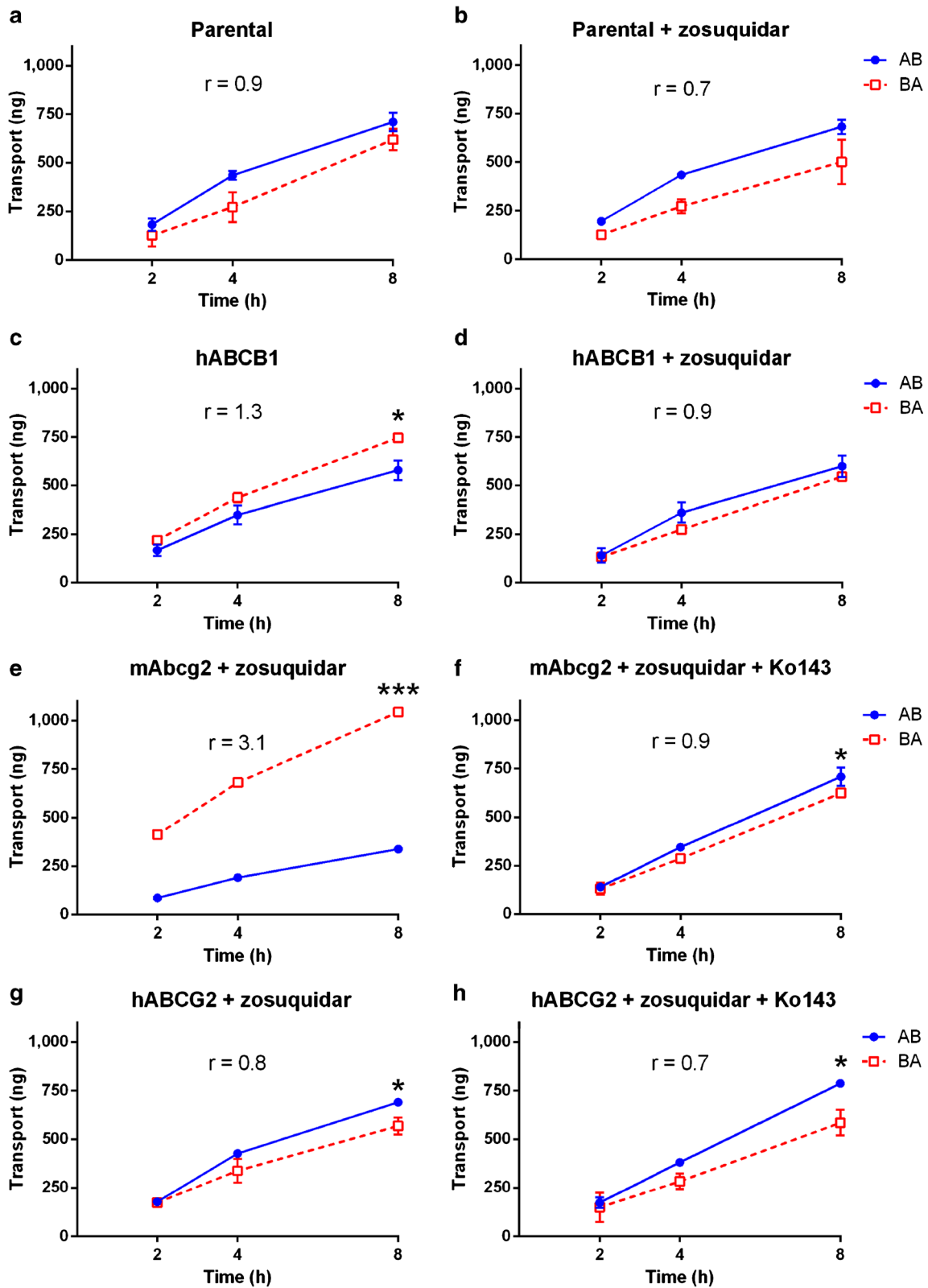
ring, regorafenib might also be a good substrate of ABCG2 and possibly ABCB1. Surprisingly, however, regorafenib is not transported by ABCG2 or ABCB1 according to the manufacturer, as tested *in vitro* using transduced LLC-MDR1 and wild-type LLC-PK1 cells, at clinically relevant concentrations ranging from 0.2 to 10 μM (6). Regorafenib was, however, found to be an inhibitor of transport of digoxin (an ABCB1 substrate) and dipyrimidole (an ABCG2 substrate) *in vitro* according to the same report. For this reason, a clinical phase I study (ClinicalTrialsGov identifier NCT02106845) is planned to investigate the interaction of regorafenib with digoxin and with rosuvastatin (another ABCG2 substrate).

CYP3A4 and UGT1A9 enzymes are responsible for the metabolism of regorafenib, resulting in two major and six minor metabolites. The formation of the two major circulating metabolites referred to as M2 (pyridine-*N*-oxide) and M5 (pyridine-*N*-oxide amide), is mediated by CYP3A4 (6). Compared to regorafenib, M2 and M5 have equal pharmacodynamic activity *in vitro* and they accumulate to similar plasma levels as regorafenib in patients once plasma steady state is reached (16,17). This accumulation is non-linear and is attributed to enterohepatic cycling and the long elimination half-life of these metabolites (6). As a consequence, the metabolites may have a significant impact on the therapeutic efficacy of regorafenib. Interestingly, even though regorafenib was not found to be transported by ABCB1 or ABCG2 *in vitro*, both M2 and M5 were found to be weakly transported substrates of ABCB1 and M5 was weakly transported by ABCG2 (7). In this study, we investigated the interaction of regorafenib and its major metabolites M2 and M5 with ABCB1, ABCG2 and CYP3A4 *in vitro* and *in vivo* in knockout mouse models.

MATERIAL AND METHODS

Chemicals

Regorafenib and zosuquidar were purchased from Sequoia Research Products (Pangbourne, UK). Zosuquidar (Eli Lilly; Indianapolis, USA) was a kind gift from Dr. O. van Tellinghen



(The Netherlands Cancer Institute, Amsterdam, The Netherlands) and Ko143 was obtained from Tocris Bioscience (Bristol, UK). Methoxyflurane (Metofane®) was obtained from Medical

Developments Australia (Melbourne, Australia). Heparin (5000 IU ml⁻¹) was obtained from Leo Pharma (Breda, The Netherlands). Bovine Serum Albumin (BSA) Fraction V,

was purchased from Roche (Mannheim, Germany). Chemicals used for the bioanalytical assay of regorafenib were described previously (18); metabolites M2 and M5 were supplied by ALSACHIM (Illkirch Graffenstaden, France). All other chemicals and reagents were obtained from Sigma-Aldrich (Steinheim, Germany).

Transport Assays

Polarized Madin-Darby Canine Kidney (MDCK-II) cell lines transduced with human (h)ABCB1, murine (m)Abcg2 and hABCG2 cDNA were used and cultured as described previously (19). Transepithelial transport assays were performed in triplicate on 12-well microporous polycarbonate membrane filters (3.0- μm pore size, Transwell 3402, Corning Inc., Lowell, MA) as described previously (20). In short, cells were allowed to grow an intact monolayer in 3 days. On day 3, cells were pre-incubated with the relevant inhibitors for 1 h. To inhibit endogenous canine *Abcb1* in the MDCK-II *Abcg2* and MDCK-II *ABCG2* cell lines, we added 5 μM zosuquidar (*ABCB1* inhibitor) to the culture medium during the entire experiment. The experiment was started by replacing the incubation medium from the donor compartment with freshly prepared drug-containing medium. At 2, 4, 8 and 24 h, 50 μl samples were collected from the acceptor compartment and stored at -30°C until analysis. The amount of transported drug was calculated after correction for volume loss due to sampling at each time point. Active transport was expressed by the transport ratio (η), which is defined as the amount of apically directed transport divided by the amount of basolaterally directed transport at a defined time point.

Animals

Male wild-type, *Abcb1a/1b*^{-/-} (21), *Abcg2*^{-/-} (22), *Abcg2*^{-/-};*Abcb1a/1b*^{-/-} (23) and *Cyp3a*^{-/-} mice (24), all of a >99% FVB genetic background were used. Mice between 9 and 13 weeks of age were used in groups of five mice per strain. The mice were kept in a temperature-controlled environment with a 12-h light/dark cycle and received a standard diet (AM-II, Hope Farms, Woerden, The Netherlands) and acidified water *ad libitum*. Animals were housed and handled according to institutional guidelines in compliance with Dutch legislation.

Drug Solutions

Regorafenib was dissolved in DMSO at 20 mg/ml and diluted 20-fold with a vehicle mixture containing 10% (v/v) polysorbate 80, 6.5% (v/v) ethanol and 2.5% (w/v) glucose in water, to obtain a 1 mg/ml solution. Regorafenib was administered orally at a dose of 10 mg/kg (10 $\mu\text{l/g}$). All working solutions were prepared freshly on the day of experiment.

Plasma and Tissue Pharmacokinetics of Regorafenib

To minimize variation in absorption, mice were fasted for 2 h prior to oral administration of regorafenib using a blunt-ended needle. For the pharmacokinetic experiment, 50 μl blood samples were drawn from the tail vein using heparin-coated capillaries (Sarstedt, Germany) at 0.5, 1, 2, 4 and 8 h. At 24 h mice were anesthetized using isoflurane and blood was collected *via* cardiac puncture. Immediately thereafter, mice were sacrificed by cervical dislocation and a set of organs was rapidly removed, weighed and subsequently frozen as whole organ at -30°C . Prior to analysis, organs were allowed to thaw and homogenized in appropriate volumes of 1% (w/v) BSA in water using a FastPrep®-24 device (MP Biomedicals, SA, California, USA). Blood samples were immediately centrifuged after collection at 2100 g for 6 min at 4°C , and plasma was collected and stored at -30°C until analysis.

Relative Accumulation of Regorafenib in Brain, Testis, Liver and Kidney

Mice were fasted for 2 h before oral gavage of regorafenib. At 0.25, 0.5 and 1 h blood was collected by tail vein sampling. At 2 h, roughly corresponding with the T_{max} , mice were anesthetized with isoflurane and blood was collected by cardiac puncture. Immediately thereafter mice were sacrificed and brain, testis, liver and kidney were removed and processed as described above. Regorafenib concentration in brain tissue was corrected for the presence of plasma in the vascular space (1.4%) (25).

Drug Analysis

Regorafenib concentration in culture medium was analyzed with a previously reported liquid-chromatography tandem mass spectrometric (LC-MS/MS) assay for regorafenib, with a calibration curve ranging from 25 to 25,000 ng/ml (18). Plasma and tissue homogenates were analyzed with an extended LC-MS/MS assay using a gradient elution, where two active metabolites were included in the previously mentioned regorafenib assay at a higher sensitivity. The calibration ranges covered 10–10,000 ng/ml with an extrapolated lower limit of detection of 5 ng/ml for both regorafenib and its metabolites (unpublished data). Tissue concentrations were accordingly corrected for their individual weights, resulting in ng regorafenib per gram tissue.

Statistics and Pharmacokinetic Calculations

The unpaired two-tailed Student's *t*-test was used to determine significant transepithelial transport for heteroscedastic data. The area under the curve (AUC) of the plasma concentration-time curve was calculated using the trapezoidal

rule, without extrapolating to infinity. The peak plasma concentration (C_{\max}) and the time to reach peak plasma concentration (T_{\max}) were determined from individual concentration-time data. Ordinary one-way analysis of variance (ANOVA) was used to determine significant differences between groups. Post-hoc Tukey's multiple comparison test was used to compare significant differences between individual groups. When variances were not homogeneously distributed, data were log-transformed before applying statistical tests. Differences were considered statistically significant when $P < 0.05$. Data are presented as mean \pm SD with each experimental group containing five mice.

RESULTS

Regorafenib is Modestly Transported by hABCB1 and Efficiently by mAbcg2 and hABCG2 *In Vitro*

Polarized MDCK-II cell lines transduced with hABCB1, mAbcg2 or hABCG2 were used to assess active transport of 5 μ M regorafenib. We observed a slight amount of basolaterally directed transport in the parental cells, presumably by endogenous as yet unidentified transporters (Fig. 1a, b). Bearing this in mind, there was a modest apically directed transport of regorafenib by hABCB1 ($r=1.3$) counteracting the basolaterally directed transport seen in the parental line as shown in Fig. 1c. This transport was inhibited by zosuquidar (Fig. 1d, $r=0.9$). Apically directed transport of regorafenib was highest in mAbcg2-expressing cells ($r=3.1$) and this transport was efficiently inhibited by Ko143 (Fig. 1e, f, $r=0.9$). In contrast to mAbcg2, hABCG2 appeared to have no effect on the transport of regorafenib (Fig. 1g, $r=0.8$). As 5 μ M regorafenib might saturate a possible modest transport activity of hABCG2, we lowered the concentration in the assay to 1 μ M. Results similar to the previous experiment were obtained for the parental, hABCB1 and mAbcg2 expressing cells, although the background basolaterally directed transport of regorafenib in the parental cells was even more pronounced, and partly also inhibited by zosuquidar (Fig. 2a-f). However, now hABCG2 showed a clear apically directed transport of regorafenib (Fig. 2g, $r=2.7$) which could be completely inhibited by Ko143 (Fig. 2h, $r=1.0$). These data suggest that hABCG2-mediated transport of regorafenib gets effectively saturated between 1 and 5 μ M in this test system.

No Substantial Effect of mAbcb1 or mAbcg2 on Plasma Pharmacokinetics of Oral Regorafenib in Mice

As regorafenib is orally administered to patients, the mice received regorafenib by oral gavage into the stomach at a dose of 10 mg/kg. The time to reach peak plasma

concentrations was about 2 h in each strain (Fig. 3). The experimental variation was quite high, and although the AUCs in the single knockout strains were significantly reduced compared to WT, to 0.8-fold in *Abcg2*^{-/-} mice ($P < 0.01$) and to 0.5-fold in *Abcb1a/1b*^{-/-} ($P < 0.001$), the combination *Abcg2*^{-/-};*Abcb1a/1b*^{-/-} mice had an AUC close to that of the WT mice. Collectively, this indicates that there is no substantial effect of these transporters on restricting the oral availability of regorafenib. This was further supported by plasma curves obtained in a subsequent short-term (2 h) oral regorafenib experiment in these mouse strains (see below).

Abcg2 and Abcb1a/1b Limit Regorafenib Brain and Testis Accumulation in Mice

Although regorafenib was largely eliminated from the plasma within 24 h, brain concentrations were increased by 4.4-fold in *Abcg2*^{-/-} mice and by 5.5-fold in *Abcg2*^{-/-};*Abcb1a/1b*^{-/-} mice compared to WT mice (Fig. 4a). Also after correction for the individual plasma concentrations and AUCs, comparable effects were seen for *Abcg2*^{-/-} and *Abcg2*^{-/-};*Abcb1a/1b*^{-/-} mice, whereas there was no effect of single *Abcb1a/1b* deficiency on brain-to-plasma ratio or brain accumulation compared to WT mice, as shown in Fig. 4b and c.

The impact of transporter proteins is especially relevant around the maximum plasma concentration. Mice were therefore sacrificed 2 h after oral administration of 10 mg/kg regorafenib. Plasma concentration curves up to 2 h were similar for all mouse strains (Fig. 5a), further confirming that the absence of *Abcg2* and/or *Abcb1a/1b* did not have a strong effect on the plasma AUC. As shown in Table I and Fig. 6a, *Abcg2* deficiency resulted in a 3.7-fold increase in regorafenib brain concentration compared to WT mice. Single *Abcb1a/1b* knockout had a small but not significant effect on brain concentration, but when both *Abcg2* and *Abcb1a/1b* were absent the brain concentration further increased to a 7.9-fold higher brain concentration compared to WT mice. This was a significant 2.1-fold increase compared to the effect of *Abcg2* deficiency alone ($P < 0.001$). Brain accumulation values (Fig. 6b) yielded essentially the same results. The data indicate that *Abcg2* has a clear effect on restricting brain accumulation of regorafenib, and *Abcb1* a modest effect that only becomes clearly apparent in the absence of *Abcg2*.

The blood-testis barrier (BTB) resembles the blood-brain barrier (BBB) with regard to the presence of *Abcg2* and *Abcb1a/1b* in the endothelial cells of blood capillaries. Therefore testis was also analyzed to assess whether regorafenib accumulation was affected by *Abcg2*, *Abcb1a/1b* or both. As shown in Fig. 6c and d, absence of *Abcg2* resulted in a 2.9-fold increase in regorafenib accumulation and additional knockout of *Abcb1a/1b* further increased regorafenib accumulation by about 1.5-fold. In contrast to the brain data, single knockout of *Abcb1a/1b* already resulted in a

significant, 2-fold increase of regorafenib accumulation in testis compared to that in wild type mice ($P < 0.01$). These results show that both *Abcg2* and *Abcb1a/1b*, alone or in combination, contribute to restricting testis accumulation of regorafenib, with *Abcg2* being the predominant transporter protein. Regorafenib concentrations in well-perfused organs like liver and kidney did not differ significantly between the strains (Supplementary Materials), indicating that *Abcg2* and *Abcb1a/1b* did not have a strong impact on the regorafenib disposition to these organs. Consequently, the relative brain accumulation of regorafenib in WT mice was about 2% of the liver accumulation, whereas brain or testis accumulation of regorafenib in the absence of *Abcg2* and *Abcb1a/1b* were increased to 17% or 30% of the liver accumulation, respectively (compare Fig. 6b and d with Supplementary Materials).

Active Regorafenib Metabolite M2 is Able to Penetrate the Brain in *Abcg2*^{-/-};*Abcb1a/1b*^{-/-} Mice

To investigate the effect of CYP3A enzymes on regorafenib metabolite formation, we administered 10 mg/kg regorafenib orally to *Cyp3a*^{-/-} mice. As shown in Fig. 5b, M2 was already detectable after 15 min, with a likely C_{max} at roughly 1–2 h in WT mice. No detectable amount of M2 was found in plasma of *Cyp3a*^{-/-} mice up to 2 h, whereas similar M2 AUCs were obtained for WT, *Abcg2*^{-/-}, *Abcb1a/1b*^{-/-} and *Abcg2*^{-/-};*Abcb1a/1b*^{-/-} mice corresponding with roughly 2% of the regorafenib AUC_{0–2}. M2 brain concentrations were below the lower limit of quantitation (LLOQ) in all mouse strains and even below the limit of detection (LOD; <5 ng/ml), with the exception of *Abcg2*^{-/-};*Abcb1a/1b*^{-/-} mice. There was therefore a minimally 2.3-fold increase in brain concentration of M2 in *Abcg2*^{-/-};*Abcb1a/1b*^{-/-} mice after 2 h compared to all the other tested mouse strains (Table I, Supplementary Materials). The amount of metabolite formed within 2 h after regorafenib administration was too low to observe BTB passage of M2, although small amounts of M2 were detectable. In liver and kidney tissue of all strains except for the *Cyp3a* knockout mice (not shown). The other active metabolite, M5, was not detected within 2 h in plasma or in the analyzed tissues. Together, the data show that formation of M2 is strongly dependent on *Cyp3a* activity in the mouse, and that M2 brain accumulation is restricted by *Abcg2* and/or *Abcb1a/1b*.

DISCUSSION

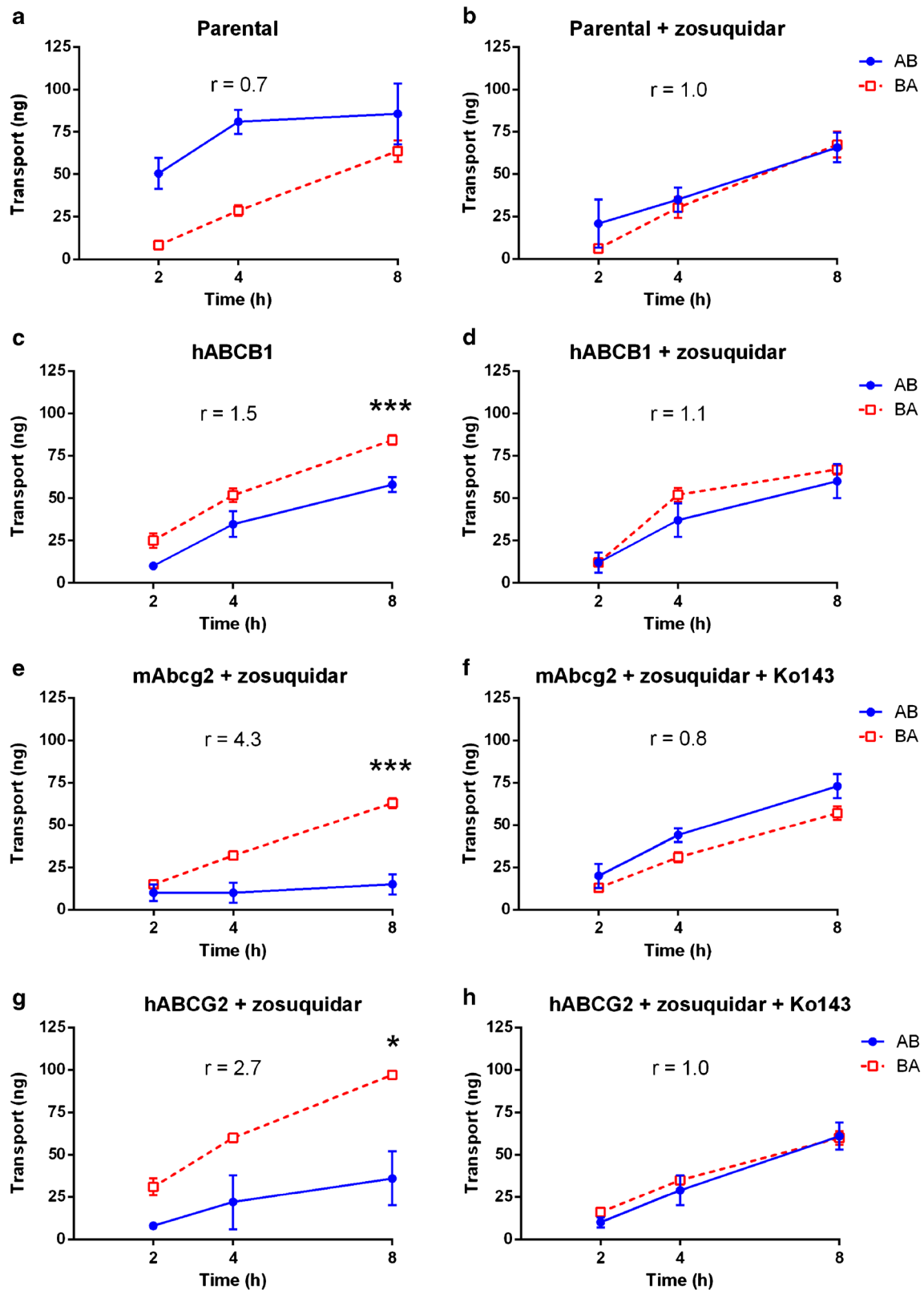
We found that regorafenib is transported by *mAbcg2* and modestly by *hABCG2* and *hABCB1*. This is evidenced *in vitro*

Fig. 2 *In vitro* transport of 1 μ M regorafenib. Transepithelial transport of regorafenib (1 μ M) was assessed in MDCK-II cells either nontransduced (a, b) or transduced with *hABCB1* (c, d), *mAbcg2* (e, f) or *hABCG2* (g, h) cDNA. At $t = 0$ h, regorafenib was applied to the donor compartment and concentrations in the acceptor compartment were measured at $t = 2, 4$ and 8 h and plotted as total amount of transport (ng) in the graphs ($n = 3$). (b, d–h) Zos. (zosuquidar, 5 μ M) and/or Ko143 (5 μ M) were applied as indicated to inhibit *hABCB1* or *hABCG2* and *mAbcg2*, respectively. r relative transport ratio. BA (□, dashed line), translocation from basolateral to apical compartment; AB (●, continuous line), translocation from apical to basolateral compartment. *, $P < 0.05$; ***, $P < 0.001$ indicates significant transepithelial transport at $t = 8$ h. Points, mean ($n = 3$); bars, SD. At $t = 8$ h, 1 nmol transport corresponds to an apparent permeability coefficient (Papp) of 3.1×10^{-5} cm/s.

by positive transport ratios and full inhibition of the apical transport by specific inhibitors. Using various knockout mouse strains, we were able to extend these findings *in vivo*. We showed that even though regorafenib oral availability was not affected by *Abcg2* or *Abcb1a/1b*, the brain and testis accumulation were clearly restricted by *Abcg2* and *Abcb1a/1b*. Lastly, we show that the active metabolite M2 is primarily formed by *Cyp3a* enzymes and was able to better penetrate the brain in the absence of both *Abcg2* and *Abcb1a/1b*, just like regorafenib.

Maximal plasma concentrations around 3.5 μ M are reached in man after a single regorafenib dose. After continuous daily dosing, regorafenib accumulates to steady state concentrations in the range of 5 to 7 μ M (16). These concentrations are in the same order of magnitude with the concentrations we found in plasma of mice (up to 12 μ M) after 10 mg/kg oral dosing *in vivo*. From this perspective, we think that our *in vivo* findings might provide a good basis for extrapolation to the clinical situation, also as regorafenib binding to mouse and human plasma proteins is similar (~99.5%) (6).

Interestingly, our *in vitro* findings contrast with what the manufacturer reported earlier. They found that regorafenib was an inhibitor of *hABCG2*, but not a transported substrate of either *hABCB1* or *hABCG2* *in vitro* using LLC-ABC1 and MDCK-II-ABC2 cell lines with concentrations ranging from 0.2 to 10 μ M (6,7,26). Although they also performed transwell membrane experiments, there may be several reasons for the discrepancy between our and their findings such as differences in assay sensitivity, transporter expression level and cell types used in these assays. From our own experience we know that it is difficult to maintain adequate *hABCG2* expression in MDCK-II cells, and studies of *hABCB1* function in LLC-PK1 cells can be compromised by the significant level of endogenous porcine ABCG2 function in these cells when the test drug (like regorafenib) is also an ABCG2 substrate. Although speculative, perhaps these factors have contributed to different outcomes of our studies and those of the manufacturer.



We found that $5 \mu\text{M}$ regorafenib was actively transported by mAbcg2 *in vitro*, while hABCG2-mediated transport was saturated at this concentration. Lowering the concentration to

$1 \mu\text{M}$ was enough to demonstrate that regorafenib was indeed a transported substrate of hABCG2. As discussed before (14,27,28), a lower *in vitro* transport capacity of hABCG2

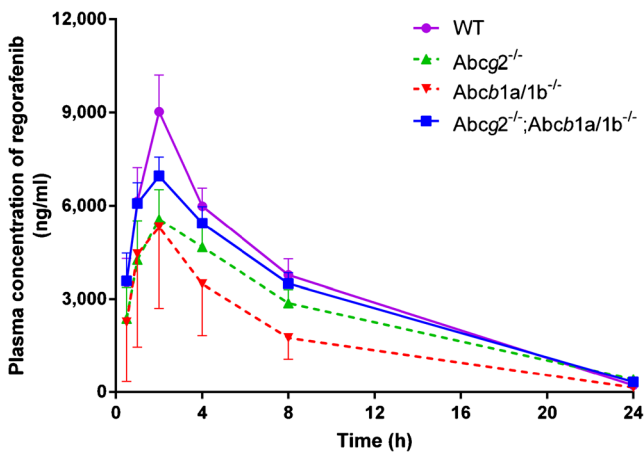


Fig. 3 Plasma concentration-time curves (AUC_{0-24}) of regorafenib in male WT (●), $Abcg2^{-/-}$ (▲), $Abcb1a/1b^{-/-}$ (▼), and $Abcg2^{-/-};Abcb1a/1b^{-/-}$ (■) mice over 24 h. Points, mean ($n=5$); bars, SD.

versus mAbcg2 that is consistently seen for many drugs in these cells may relate to the difficulty in obtaining MDCKII cell lines with a high hABCG2 expression and activity. Another possibility is that the K_m of regorafenib for hABCG2 is lower than that for mAbcg2. In line with the *in vitro* results, we found a substantial impact of mAbcg2 *in vivo* at the BBB at plasma concentrations in the clinical range of up to $\sim 12 \mu M$ regorafenib. In addition, Uchida *et al.* demonstrated that hABCG2 is 1.9-fold more expressed in human brain microvessels than mAbcg2 in the murine brain (29). Therefore the role of hABCG2 in the brain disposition of regorafenib could be even more pronounced in man than we found in the mouse.

Our findings show that regorafenib is a moderate $Abcb1a/1b$ and a good $Abcg2$ substrate at the BBB. Absence of $Abcb1a/1b$ did not affect the brain disposition of regorafenib at the C_{max} ($t=2$ h), while deficiency of $Abcg2$ led to a 3.6-fold increase in brain accumulation. However, the additional contribution of $Abcb1a/1b$ for the brain accumulation became apparent in the

absence of both transporters, leading to an 8.2-fold increase. This disproportionate effect is seen more often for TKIs and other drugs that are shared $Abcg2$ and $Abcb1$ substrates and is well explained by various published theoretical pharmacokinetic models (30–32).

Regorafenib is one of the very few TKIs (including sorafenib and CYT387) whose brain disposition is dominated by $Abcg2$ and not by $Abcb1a$, whereas their oral availability was not affected by the absence of these transporters (13,14,33). Brain accumulation of the majority of the TKIs and other targeted anti-cancer drugs tested so far were shown to be affected mainly or only by $Abcb1a/1b$ deficiency such as axitinib (12), cediranib (34), crizotinib (35), everolimus (36), trametinib (37) and veliparib (38). One of the reasons for this is likely to be the approximately 3 to 4-fold higher expression of $Abcb1a$ protein compared to $Abcg2$ at the mouse BBB (39,40), further emphasizing the good substrate specificity of $Abcg2$ for regorafenib. Although regorafenib has high structural similarity to sorafenib, regorafenib seems to have a better oral bioavailability and a more delayed T_{max} compared to sorafenib in patients, whereas several other pharmacokinetic parameters seem to be similar (Supplementary Materials) (17,41).

In this study, we observed a clear impact of context-dependency in ABC transporter activity. We found that absence of $Abcb1a/1b$ and $Abcg2$ does not affect oral availability, but does influence brain and testis accumulation of regorafenib. Similar effects have been described previously for example with sorafenib, sunitinib and CYT387 (14,28,33). Additionally, we found a significant detectable impact of single $Abcb1a/1b$ knockout on the regorafenib accumulation in the testis, while there was a slight but insignificant impact of $Abcb1a/1b$ absence in the brain. This could perhaps be attributed to the relatively lower amount of mAbcg2 present in testis compared to the brain in mice (42), whereas intrinsic differences in tightness of the BTB

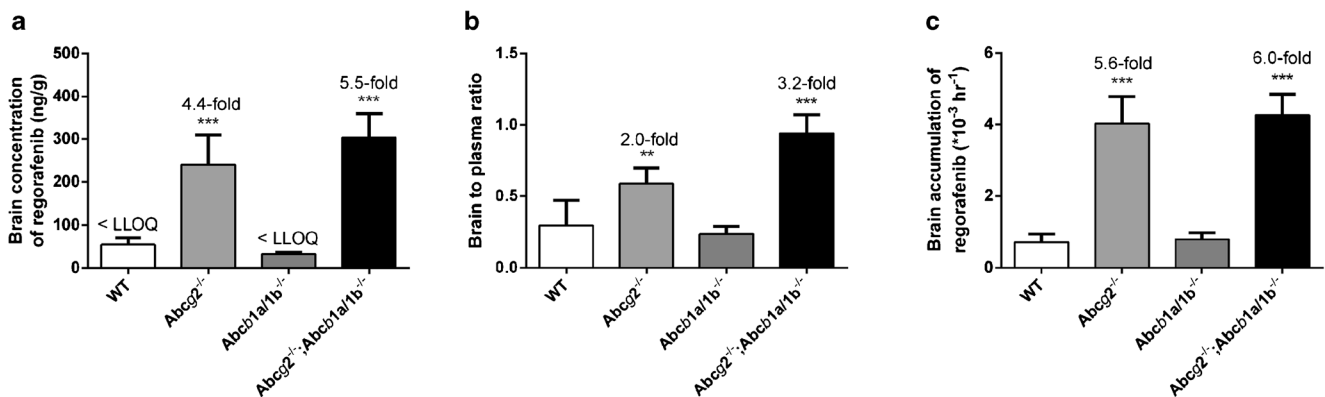


Fig. 4 Brain concentration (a), brain-to-plasma ratios (b) and relative brain accumulation (c) of regorafenib in male WT, $Abcg2^{-/-}$, $Abcb1a/1b^{-/-}$ and $Abcg2^{-/-};Abcb1a/1b^{-/-}$ mice 24 h after oral administration of 10 mg/kg regorafenib. **, $P < 0.01$; ***, $P < 0.001$ compared with WT mice. Data are presented as mean \pm SD ($n=5$). Where necessary, data were log-transformed to normalize the SDs between study groups.

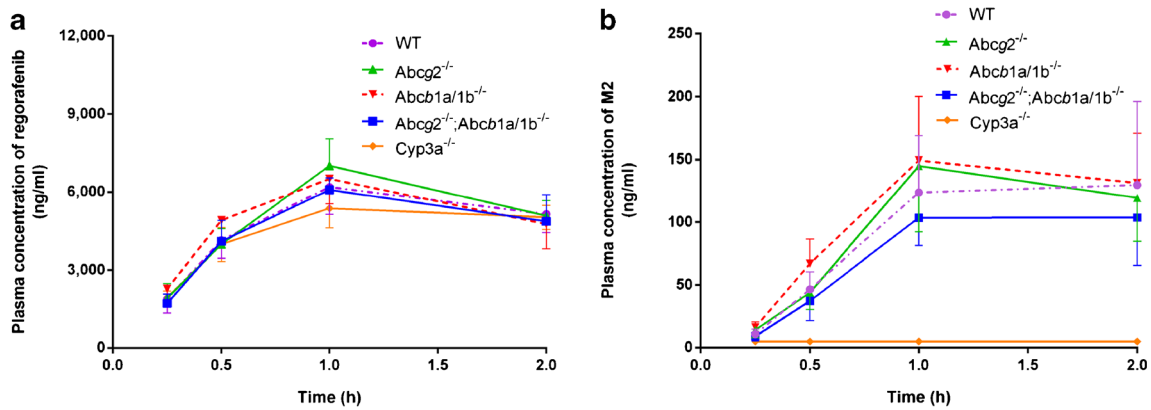


Fig. 5 Plasma concentration-time curves (AUC₀₋₂) of regorafenib (a) and metabolite M2 (b) in male WT (●), Abcg2^{-/-} (▲), Abcb1a/1b^{-/-} (▼), Abcg2^{-/-};Abcb1a/1b^{-/-} (■) and Cyp3a^{-/-} (◆) mice over 2 h after oral administration of 10 mg/kg regorafenib. Points, mean (n = 5); bars, SD.

versus BBB may also have played a role in their slightly different behavior (43).

Unlike M5, formation of M2 appears to be fast and solely mediated by Cyp3a enzymes in the mouse. We were able to measure M2 already 15 min after oral administration of regorafenib in all strains except for

the Cyp3a knockout mice, whereas we could not detect M5 after 2 h. As trace amounts of M2, only slightly above LOD, were measured in the brain of Abcg2^{-/-}; Abcb1a/1b^{-/-} mice, it is likely that M2 is also a substrate of one or both of these transporters. We think that the single bolus administration of regorafenib was

Table 1 Pharmacokinetic Parameters of Regorafenib and the Metabolite M2, 2 and 24 h after Oral Administration of 10 mg/kg Regorafenib to Male Wild-Type, Abcg2^{-/-}, Abcb1a/1b^{-/-}, Abcg2^{-/-};Abcb1a/1b^{-/-} and Cyp3a^{-/-} Mice

Parameter	Genotype	Genotype				
		Wild-type	Abcg2 ^{-/-}	Abcb1a/1b ^{-/-}	Abcg2 ^{-/-} ;Abcb1a/1b ^{-/-}	Cyp3a ^{-/-}
Plasma AUC ₍₀₋₂₄₎ (μg*h/ml)	Regorafenib	77 ± 8	59 ± 8**	42 ± 11***	71 ± 5	
C _{max} (μg/ml)	24 h	9.0 ± 1.2	5.6 ± 1.0	6.5 ± 1.7	7.0 ± 0.6	
T _{max} (h)		2	2	1-4	2	
C _{brain} (ng/g)		55 ± 15 [#]	240 ± 69***	32 ± 5* ^{+++,#}	303 ± 56***	
Fold increase C _{brain}		1.0	4.4	0.6	5.5	
P _{brain} (*10 ⁻³ h ⁻¹)		0.7 ± 0.2	4.0 ± 0.8***	0.8 ± 0.2 ⁺⁺⁺	4.3 ± 0.6***	
Fold increase P _{brain}		1.0	5.6	1.1	6.0	
Plasma AUC ₍₀₋₂₎ (μg*h/ml)	Regorafenib	9.2 ± 1.3	9.8 ± 1.2	9.7 ± 1.4	9.0 ± 1.0	8.5 ± 0.8
C _{max} (μg/ml)	2 h	6.2 ± 1.0	7.0 ± 1.0	6.5 ± 1.0	6.1 ± 0.5	5.5 ± 0.5
T _{max} (h)		1-2	1	1	1	1-2
C _{brain} (ng/g)		482 ± 112	1808 ± 161*** ⁺⁺	689 ± 104 ⁺⁺⁺	3804 ± 585***	522 ± 199
Fold increase C _{brain}		1.0	3.7	1.4	7.9	1.1
P _{brain} (*10 ⁻³ h ⁻¹)		52 ± 11	188 ± 33*** ⁺⁺	72 ± 10 ⁺⁺⁺	428 ± 78***	66 ± 26
Fold increase P _{brain}		1.0	3.6	1.4	8.2	1.3
Plasma AUC ₍₀₋₂₎ (ng*h/ml)	M2	178 ± 68	188 ± 62	207 ± 65	146 ± 37	<9 [#]
C _{max} (ng/ml)	2 h	143 ± 61	145 ± 53	150 ± 51	115 ± 27	<5 [#]
T _{max} (h)		1-2	1	1-2	1-2	n.a.
C _{brain} (ng/g)		<14 [#]	<14 [#]	<13 [#]	33 ± 14	<15 [#]
P _{brain} (*10 ⁻³ h ⁻¹)		n.a.	n.a.	n.a.	226 ± 79	n.a.

AUC area under the plasma concentration-time curve, C_{max} maximum drug concentration in plasma, T_{max} the time (h) after drug administration needed to reach maximum plasma concentration, C_{brain} brain concentration, P_{brain} brain accumulation (brain concentration divided by AUC), n.a. not applicable

* P < 0.05; ** P < 0.01; *** P < 0.001 compared to WT mice and + P < 0.05; ++ P < 0.01; +++ P < 0.001 compared to Abcg2^{-/-}; Abcb1a/1b^{-/-} mice (WT and Cyp3a^{-/-}) significance data for this last comparison are not shown; [#] maximal value, calculated with the lower limit of detection in the used LC-MS/MS assay (5 ng/ml) or with the extrapolated value where possible. Data are given as mean ± SD (n = 5)

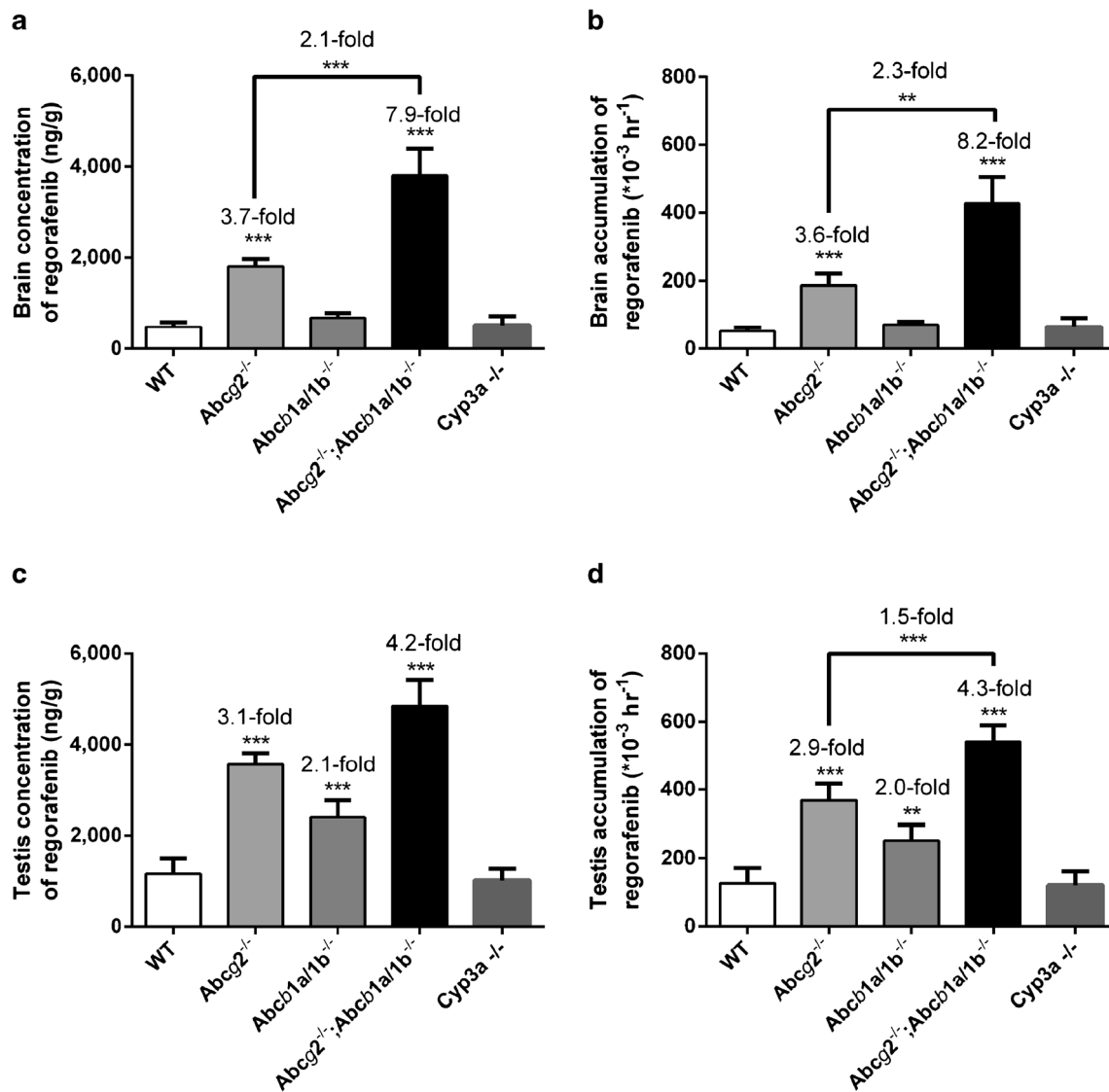


Fig. 6 Brain concentration (a), relative brain accumulation (b), testis concentration (c) and testis accumulation (d) of regorafenib in male WT, *Abcg2*^{+/-}, *Abcb1a/1b*^{+/-}, *Abcg2*^{+/-};*Abcb1a/1b*^{+/-} and *Cyp3a*^{-/-} mice, 2 h after oral administration of 10 mg/kg regorafenib. **, $P < 0.01$; ***, $P < 0.001$ compared with WT mice. Data are presented as mean \pm SD ($n = 5$). Where necessary, data were log-transformed to normalize the SDs between study groups.

not enough to result in reliably detectable levels of M2 and M5. Also in patients substantial levels of M2 and M5 are detectable after subsequent daily oral administrations of regorafenib (17,41).

In spite of several performed clinical trials, none have yet systematically assessed the efficacy of regorafenib in central nervous system (CNS) metastases. We think that our findings can be a good source for future clinical studies of cancer patients with CNS involvement, as we here showed a clear impact of ABCB1 and ABCG2 in restricting brain penetration of regorafenib. Moreover, based on our previous experience (14,20,28), we suggest that combined administration of regorafenib with ABCB1 and ABCG2 inhibitors such as elacridar might improve the brain concentration and

thus efficacy of regorafenib against metastases located behind an intact BBB.

CONCLUSION

We conclude that the multikinase inhibitor regorafenib is transported well by hABCG2 and mAbcg2, and modestly by hABCB1 *in vitro*. This is supported *in vivo* in mice where brain and testis accumulation are restricted mostly by *Abcg2* and additionally by *Abcb1*. These results indicate that co-administration of ABCG2 and/or ABCB1 inhibitors may increase exposure of regorafenib and its active M2 metabolite in patients, thus providing an option to

better treat (micro)metastases behind a functionally intact blood–brain barrier.

ACKNOWLEDGMENTS AND DISCLOSURES

The research group of A.H. Schinkel receives revenue from commercial distribution of some of the mouse strains used in this study.

Anita Kort and Selvi Durmus contributed equally.

REFERENCES

1. Schinkel AH, Wagenaar E, Mol CA, van Deemter L. P-glycoprotein in the blood–brain barrier of mice influences the brain penetration and pharmacological activity of many drugs. *J Clin Invest.* 1996;97(11):2517–24.
2. Chen Y, Agarwal S, Shaik NM, Chen C, Yang Z, Elmquist WF. P-glycoprotein and breast cancer resistance protein influence brain distribution of dasatinib. *J Pharmacol Exp Ther.* 2009;330(3):956–63.
3. Noguchi K, Katayama K, Sugimoto Y. Human ABC transporter ABCG2/BCRP expression in chemoresistance: basic and clinical perspectives for molecular cancer therapeutics. *Pharmacogenomics Pers Med.* 2014;7:53–64.
4. Wilhelm SM, Dumas J, Adnane L, Lynch M, Carter CA, Schutz G, *et al.* Regorafenib (BAY 73-4506): a new oral multikinase inhibitor of angiogenic, stromal and oncogenic receptor tyrosine kinases with potent preclinical antitumor activity. *Int J Cancer.* 2011;129(1):245–55.
5. Grothey A, Van Cutsem E, Sobrero A, Siena S, Falcone A, Ychou M, *et al.* Regorafenib monotherapy for previously treated metastatic colorectal cancer (CORRECT): an international, multicentre, randomised, placebo-controlled, phase 3 trial. *Lancet.* 2013;381(9863):303–12.
6. Center for Drug Evaluation and Research of the US Department of Health and Human Services, Food and Drug Administration. Clinical pharmacology and biopharmaceutics review(s). 2014 June 5. Available from: http://www.accessdata.fda.gov/drugsatfda_docs/nda/2012/203085Orig1s000ClinPharmR.pdf.
7. European Medicines Agency. Stivarga summary of product characteristics. 2014 September 24. Available from: http://www.ema.europa.eu/docs/en_GB/document_library/EPAR_-_Product_Information/human/002573/WC500149164.pdf.
8. Demetri GD, Reichardt P, Kang YK, Blay JY, Rutkowski P, Gelderblom H, *et al.* Efficacy and safety of regorafenib for advanced gastrointestinal stromal tumours after failure of imatinib and sunitinib (GRID): an international, multicentre, randomised, placebo-controlled, phase 3 trial. *Lancet.* 2013;381(9863):295–302.
9. Sallinen H, Anttila M, Grohn O, Koponen J, Hamalainen K, Kholova I, *et al.* Cotargeting of VEGFR-1 and -3 and angiotensin receptor Tie2 reduces the growth of solid human ovarian cancer in mice. *Cancer Gene Ther.* 2011;18(2):100–9.
10. Tsai JH, Lee WM. Tie2 in tumor endothelial signaling and survival: implications for antiangiogenic therapy. *Mol Cancer Res.* 2009;7(3):300–10.
11. Bruix J, Tak WY, Gasbarrini A, Santoro A, Colombo M, Lim HY, *et al.* Regorafenib as second-line therapy for intermediate or advanced hepatocellular carcinoma: multicentre, open-label, phase II safety study. *Eur J Cancer.* 2013;49(16):3412–9.
12. Poller B, Iusuf D, Sparidans RW, Wagenaar E, Beijnen JH, Schinkel AH. Differential impact of P-glycoprotein (ABCB1) and breast cancer resistance protein (ABCG2) on axitinib brain accumulation and oral plasma pharmacokinetics. *Drug Metab Dispos.* 2011;39(5):729–35.
13. Agarwal S, Sane R, Ohlfest JR, Elmquist WF. The role of the breast cancer resistance protein (ABCG2) in the distribution of sorafenib to the brain. *J Pharmacol Exp Ther.* 2011;336(1):223–33.
14. Lagas JS, van Waterschoot RA, Sparidans RW, Wagenaar E, Beijnen JH, Schinkel AH. Breast cancer resistance protein and P-glycoprotein limit sorafenib brain accumulation. *Mol Cancer Ther.* 2010;9(2):319–26.
15. Hu S, Chen Z, Franke R, Orwick S, Zhao M, Rudek MA, *et al.* Interaction of the multikinase inhibitors sorafenib and sunitinib with solute carriers and ATP-binding cassette transporters. *Clin Cancer Res.* 2009;15(19):6062–9.
16. Zopf D, Heinig R, Thierauch KH, Hirth-Dietrich C, Hafner F, Christensen O, Lin T, Wilhelm S, Radtke M. Regorafenib (BAY 73-4506): preclinical pharmacology and clinical identification and quantification of its major metabolites [abstract]. In: Proceedings of the 101st Annual Meeting of the American Association for Cancer Research. Washington DC, Philadelphia (PA): Cancer Res; 2010 Apr 17–21. p. Suppl.
17. Mross K, Frost A, Steinbild S, Hedbom S, Buchert M, Fasol U, *et al.* A phase I dose-escalation study of regorafenib (BAY 73-4506), an inhibitor of oncogenic, angiogenic, and stromal kinases, in patients with advanced solid tumors. *Clin Cancer Res.* 2012;18(9):2658–67.
18. Luetthi D, Durmus S, Schinkel AH, Schellens JH, Beijnen JH, Sparidans RW. Liquid chromatography-tandem mass spectrometric assay for the multikinase inhibitor regorafenib in plasma. *Biomed Chromatogr.* 2014.
19. Evers R, Kool M, van Deemter L, Janssen H, Calafat J, Oomen LC, *et al.* Drug export activity of the human canalicular multispecific organic anion transporter in polarized kidney MDCK cells expressing cMOAT (MRP2) cDNA. *J Clin Invest.* 1998;101(7):1310–9.
20. Durmus S, Sparidans RW, Wagenaar E, Beijnen JH, Schinkel AH. Oral availability and brain penetration of the B-RAFV600E inhibitor vemurafenib can be enhanced by the P-glycoprotein (ABCB1) and breast cancer resistance protein (ABCG2) inhibitor elacridar. *Mol Pharm.* 2012;9(11):3236–45.
21. Schinkel AH, Mayer U, Wagenaar E, Mol CA, van Deemter L, Smit JJ, *et al.* Normal viability and altered pharmacokinetics in mice lacking mdr1-type (drug-transporting) P-glycoproteins. *Proc Natl Acad Sci U S A.* 1997;94(8):4028–33.
22. Jonker JW, Buitelaar M, Wagenaar E, Van Der Valk MA, Scheffer GL, Scheper RJ, *et al.* The breast cancer resistance protein protects against a major chlorophyll-derived dietary phototoxin and protoporphyria. *Proc Natl Acad Sci U S A.* 2002;99(24):15649–54.
23. Jonker JW, Merino G, Musters S, van Herwaarden AE, Bolscher E, Wagenaar E, *et al.* The breast cancer resistance protein BCRP (ABCG2) concentrates drugs and carcinogenic xenotoxins into milk. *Nat Med.* 2005;11(2):127–9.
24. van Waterschoot RA, Lagas JS, Wagenaar E, van der Kruijssen CM, van Herwaarden AE, Song JY, *et al.* Absence of both cytochrome P450 3A and P-glycoprotein dramatically increases docetaxel oral bioavailability and risk of intestinal toxicity. *Cancer Res.* 2009;69(23):8996–9002.
25. Dai H, Marbach P, Lemaire M, Hayes M, Elmquist WF. Distribution of STI-571 to the brain is limited by P-glycoprotein-mediated efflux. *J Pharmacol Exp Ther.* 2003;304(3):1085–92.
26. Pharmaceuticals and Medical Devices Agency Japan. Review report on Stivarga. 2014 June 5. Available from: http://www.pmda.go.jp/english/service/pdf/drugs/stivarga_mar2010_e.pdf.
27. Tang SC, de Vries N, Sparidans RW, Wagenaar E, Beijnen JH, Schinkel AH. Impact of P-glycoprotein (ABCB1) and breast cancer resistance protein (ABCG2) gene dosage on plasma pharmacokinetics and brain accumulation of dasatinib, sorafenib, and sunitinib. *J Pharmacol Exp Ther.* 2013;346(3):486–94.

28. Tang SC, Lankheet NA, Poller B, Wagenaar E, Beijnen JH, Schinkel AH. P-glycoprotein (ABCB1) and breast cancer resistance protein (ABCG2) restrict brain accumulation of the active sunitinib metabolite N-desethyl sunitinib. *J Pharmacol Exp Ther*. 2012;341(1):164–73.
29. Uchida Y, Ohtsuki S, Katsukura Y, Ikeda C, Suzuki T, Kamiie J, et al. Quantitative targeted absolute proteomics of human blood–brain barrier transporters and receptors. *J Neurochem*. 2011;117(2):333–45.
30. Kalvass JC, Pollack GM. Kinetic considerations for the quantitative assessment of efflux activity and inhibition: implications for understanding and predicting the effects of efflux inhibition. *Pharm Res*. 2007;24(2):265–76.
31. Zamek-Gliszczynski MJ, Kalvass JC, Pollack GM, Brouwer KL. Relationship between drug/metabolite exposure and impairment of excretory transport function. *Drug Metab Dispos*. 2009;37(2):386–90.
32. Kodaira H, Kusuhara H, Ushiki J, Fuse E, Sugiyama Y. Kinetic analysis of the cooperation of P-glycoprotein (P-gp/Abcb1) and breast cancer resistance protein (Bcrp/Abcg2) in limiting the brain and testis penetration of erlotinib, flavopiridol, and mitoxantrone. *J Pharmacol Exp Ther*. 2010;333(3):788–96.
33. Durmus S, Xu N, Sparidans RW, Wagenaar E, Beijnen JH, Schinkel AH. P-glycoprotein (MDR1/ABCB1) and breast cancer resistance protein (BCRP/ABCG2) restrict brain accumulation of the JAK1/2 inhibitor, CYT387. *Pharmacol Res*. 2013;76:9–16.
34. Wang T, Agarwal S, Elmquist WF. Brain distribution of cediranib is limited by active efflux at the blood–brain barrier. *J Pharmacol Exp Ther*. 2012;341(2):386–95.
35. Chuan Tang S, Nguyen LN, Sparidans RW, Wagenaar E, Beijnen JH, Schinkel AH. Increased oral availability and brain accumulation of the ALK inhibitor crizotinib by coadministration of the P-glycoprotein (ABCB1) and breast cancer resistance protein (ABCG2) inhibitor elacridar. *Int J Cancer*. 2014;134(6):1484–94.
36. Tang SC, Sparidans RW, Cheung KL, Fukami T, Durmus S, Wagenaar E, et al. P-glycoprotein, CYP3A, and plasma carboxylesterase determine brain and blood disposition of the mTOR Inhibitor everolimus (Afinitor) in mice. *Clin Cancer Res*. 2014;20(12):3133–45.
37. Vaidhyanathan S, Mittapalli RK, Sarkaria JN, Elmquist WF. Factors influencing the CNS distribution of a novel MEK-1/2 inhibitor: implications for combination therapy for melanoma brain metastases. *Drug Metab Dispos*. 2014;42(8):1292–300.
38. Lin F, de Gooijer MC, Roig EM, Buil LC, Christner SM, Beumer JH, et al. ABCB1, ABCG2, and PTEN determine the response of glioblastoma to temozolomide and ABT-888 therapy. *Clin Cancer Res*. 2014;20(10):2703–13.
39. Agarwal S, Hartz AM, Elmquist WF, Bauer B. Breast cancer resistance protein and P-glycoprotein in brain cancer: two gatekeepers team up. *Curr Pharm Des*. 2011;17(26):2793–802.
40. Kamiie J, Ohtsuki S, Iwase R, Ohmine K, Katsukura Y, Yanai K, et al. Quantitative atlas of membrane transporter proteins: development and application of a highly sensitive simultaneous LC/MS/MS method combined with novel in-silico peptide selection criteria. *Pharm Res*. 2008;25(6):1469–83.
41. Strumberg D, Clark JW, Awada A, Moore MJ, Richly H, Hendlisz A, et al. Safety, pharmacokinetics, and preliminary antitumor activity of sorafenib: a review of four phase I trials in patients with advanced refractory solid tumors. *Oncologist*. 2007;12(4):426–37.
42. Dankers AC, Sweep FC, Pertijs JC, Verweij V, van den Heuvel JJ, Koenderink JB, et al. Localization of breast cancer resistance protein (Bcrp) in endocrine organs and inhibition of its transport activity by steroid hormones. *Cell Tissue Res*. 2012;349(2):551–63.
43. Holash JA, Harik SI, Perry G, Stewart PA. Barrier properties of testis microvessels. *Proc Natl Acad Sci U S A*. 1993;90(23):11069–73.